Color gradients of spiral disks in the Sloan Digital Sky Survey *

Cheng-Ze Liu[1,2,3,4], Shi-Yin Shen[1,3], Zheng-Yi Shao[1,3], Rui-Xiang Chang[1,3],
Jin-Liang Hou[1], Jun Yin[1,2] and Da-Wei Yang[4]

[1] Key Laboratory for Research in Galaxies and Cosmology, Shanghai Astronomical Observatory,
   Chinese Academy of Sciences, Shanghai 200030, China; *czliu@shao.ac.cn*
[2] Graduate University of Chinese Academy of Sciences, Beijing 100049, China
[3] Key Laboratory for Astrophysics, Shanghai 200234, China
[4] Department of Physics, Hebei Normal University, Shijiazhuang 050016, China

Abstract   We investigate the radial color gradients of galactic disks using a sample
of $\sim 20\,000$ face-on spiral galaxies selected from the fourth data release of the Sloan
Digital Sky Survey (SDSS-DR4). We combine galaxies with similar concentrations, sizes
and luminosities to construct *composite* galaxies, and then measure their color profiles
by stacking the azimuthally averaged radial color profiles of all the member galaxies.
Except for the smallest galaxies ($R_{50} < 3\,\text{kpc}$), almost all galaxies show negative disk
color gradients with mean $g - r$ gradient $\bar{G}_{\text{gr}} = -0.006\,\text{mag}\,\text{kpc}^{-1}$ and $r - z$ gradient
$\bar{G}_{\text{rz}} = -0.018\,\text{mag}\,\text{kpc}^{-1}$. The disk color gradients are independent of the morphologi-
cal types of galaxies and strongly dependent on the disk surface brightness μ_{d}, with lower
surface brightness galactic disks having steeper color gradients. We quantify the intrinsic
correlation between color gradients and surface brightness as $G_{\text{gr}} = -0.011\mu_{\text{d}} + 0.233$
and $G_{\text{rz}} = -0.015\mu_{\text{d}} + 0.324$. These quantified correlations provide tight observational
constraints on the formation and evolution models of spiral galaxies.

Key words: galaxies: spiral — galaxies: statistics — galaxies: evolution — galaxies:
fundamental parameters (color gradient, luminosity, radius, surface brightness)

1 INTRODUCTION

The radial color gradient of a spiral galaxy freezes its fossil information about the star formation history
along the disk and therefore provides a strong constraint on the models of disk formation and evolution.
Earlier studies revealed that most spiral galaxies show negative color gradients, i.e. the color is gradually
bluer from the center outwards (e.g., Kim & Ann 1990; de Jong 1996c; Bell & de Jong 2000; Gadotti &
dos Anjos 2001; MacArthur et al. 2004; Taylor et al. 2005).

   Kim & Ann (1990) studied the radial color distributions of a sample of 103 face-on galaxies with
different morphological types. They concluded that about 40 percent of elliptical and lenticular galaxies
and about 75 percent of intermediate type spiral galaxies show clear negative color gradients, while the
latest type spiral and irregular galaxies have positive gradients or no gradient at all. For spiral galaxies,
they found a weak correlation between the color gradient and absolute magnitude, with more luminous
spirals having steeper gradients. However, in their work, the color gradient was measured along the
whole image of each galaxy, where the bulge and disk components were not decomposed.

It is well established that a spiral galaxy can be decomposed into a concentrated bulge plus an exponential disk (de Vaucouleurs 1959; Simien & Michard 1990; Capaccioli et al. 1992). Therefore, the negative color gradient of a spiral galaxy might have partially originated from the configuration of these two components. To remove this effect and measure the color gradients of these two components separately, a bulge-disk decomposition is required. de Jong (1996a,b,c) made the bulge-disk decomposition for a sample of 86 face-on spiral galaxies and investigated radial color distributions of disk components in optical and near-infrared bands. He found that the color of a disk component also becomes bluer from the center outwards, but no significant correlations were found between the color gradients and other structural parameters of galaxies, such as the color, inclination, morphological type, central surface brightness, scale-length, integrated magnitude and so on. However, the decomposition is dependent on the models used. Different models used could give different results. Alternatively, Taylor et al. (2005) investigated the color gradients of the bulge dominated inner parts and the disk dominated outer parts of 142 galaxies by simply separating each galaxy at the effective radius R_e. For the disk parts, they found that the early and intermediate type spiral galaxies show weak negative color gradients, while the late type spiral and irregular galaxies have positive color gradients.

Although the color gradient has been extensively investigated, its quantitative definitions are still diverse in different studies. There are mainly two branches of such definitions. One is the color variation ΔCI as a function of scaled radius (e.g., scale-length R_d, half-light radius R_{50}), either in linear space (Kim & Ann 1990; Taylor et al. 2005) or in logarithmic space (Tamura & Ohta 2003; Wu et al. 2005; Li et al. 2005). This kind of definition implies that galaxies with different sizes have similarities in the structure of their color distributions. The other branch is the ΔCI measured along the physical radius, e.g. the color variation per kpc (Moth & Elston 2002; Muñoz-Mareos et al. 2007), which could also be presented in either linear or logarithmic space. Additionally, if one assumes that the galactic disk in different wavebands could all be well modeled by exponential profiles, the change of scale-length as a function of waveband could also be used to parameterize the color gradient (Peletier et al. 1994; de Jong 1996c; Cunow 2004). Despite the diversity of definitions, the color gradient is an essential parameter that quantifies the systematic change of the color profile of a galaxy.

To derive the color profile of a galaxy, detailed photometric analyses in different wavebands are required. Moreover, to get robust conclusions about the correlations between color gradients and other structural parameters, a large and homogenous sample of galaxies is needed. Up to now, the number of galaxies with detailed measurements of color profiles is quite limited (Gadotti & dos Anjos 2001; Pohlen & Trujillo 2006; Muñoz-Mareos et al. 2007; Azzollini et al. 2008). On the other hand, the Sloan Digital Sky Survey (SDSS, York et al. 2000) has surveyed about a quarter of the whole sky in 5 broad wavebands (u, g, r, i, z) and provided a large catalog of photometric data of galaxies (Adelman-McCarthy et al. 2007). In the released catalog, the surface brightness profile of each galaxy has been measured in a series of fixed concentric annuli, known as *profMean*[1] (see Stoughton et al. 2002 for detail, hereafter EDR). Due to the short exposure time (about 54 s) of an SDSS image, the signal-to-noise ratio (S/N) of *profMean* data is limited and it is suggested to only be used in the cumulative profile for individual galaxies in the EDR paper[2]. However, the S/N could be greatly improved by stacking the profiles (*profMean*) of a large number of similar galaxies. The large amount of galaxies in SDSS provides an opportunity to make subsamples with enough member galaxies for such stacking. Compared to the direct image stacking methods with contaminated sources carefully masked (e.g. Zibetti et al. 2004; de Jong 2008; Hathi et al. 2008), this kind of catalog data stacking is more vulnerable to background contaminations, but is much simpler and more suitable for the analysis of large data sets (Azzollini et al. 2008; Bakos et al. 2008).

In this study, we use a large sample of face-on spiral galaxies ($\sim 20\,000$) selected from SDSS-DR4 (Adelman-McCarthy et al. 2006) to statistically investigate their disk color gradients. We divide these spiral galaxies into subsamples with similar concentrations, sizes and luminosities, and then construct

---

[1] Before calculating the surface brightness profile *profMean*, the foreground and background objects have been deblended by the FRAMES pipeline, see Lupton et al. (2001) and Stoughton et al. (2002).

[2] Blanton et al. (2003b) has used *profMean* and successfully fitted the surface brightness profile with a Sersic model for each individual galaxy.

composite galaxies by combining the color profiles of the member galaxies in each subsample. After measuring the color gradients of disk components of these *composite* galaxies, we further explore possible correlations between color gradients and structural parameters. The main aim of this work is to find out which parameter is primarily correlated with the color gradient and discuss its physical implications.

The structure of this paper is as follows. In Section 2, we describe our sample selection and the building of *composite* galaxies. The color gradients and their correlations with other structural parameters are presented in Section 3. Finally, we give a brief summary and discussions in Section 4.

2 DATA

2.1 Sampling

The galaxies used in this paper were drawn from the main galaxy sample of the SDSS-DR4, which is a spectroscopic sample complete to r-band Petrosian magnitudes $r_P < 17.77$ (Strauss et al. 2002). We use galaxies with $r_P < 17.5$ and redshifts $z > 0.01$. The magnitude limit excludes faint objects, ensuring that the structures of the galaxies are nicely resolved by SDSS images (Desroches et al. 2007). The low redshift limit eliminates the effect of peculiar velocity on distance estimation.
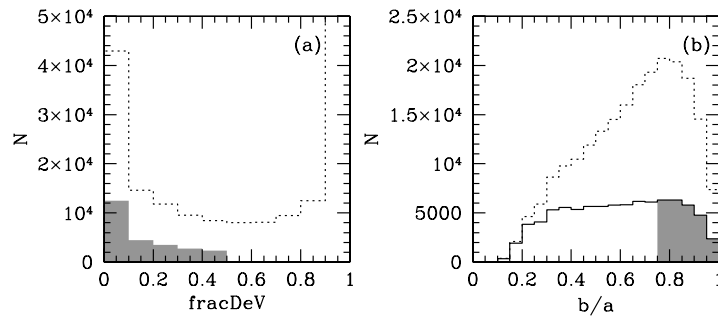
Fig. 1 Histograms of *fracDeV* (*left panel*) and axis ratio b/a (*right panel*). The dotted histograms show the distributions of the initial sample with $r_P < 17.5$ and $z > 0.01$ while the shadowed regions represent the distributions of the final sample of 25 517 face-on spiral galaxies ($r_P < 17.5$, $z > 0.01$, *fracDeV*< 0.5 and $b/a > 0.75$). The solid histogram in the right panel shows the b/a distribution of selected spiral galaxies (*fracDeV*< 0.5), see text for detail.

To select spiral galaxies, we adopt the criterion *fracDeV*< 0.5 (in r-band [3]). The parameter *fracDeV* indicates the likelihood of the surface brightness profile that can be best modeled by a de Vaucouleurs profile (Abazajian et al. 2004) and has been widely used as a galaxy morphology indicator (e.g., Bernardi et al. 2005; Chang et al. 2006; Shao et al. 2007; Padilla & Strauss 2008; Zhong et al. 2008). Strateva et al. (2001) have shown that the criterion *fracDeV*< 0.5 can separate late type galaxies from early type ones with a reliability of ~ 90 percent. We show the histogram of *fracDeV* of sample galaxies in the left panel of Figure 1. As we can see, for the galaxies with *fracDeV*< 0.5, most of them peak at *fracDeV*~ 0.

Aiming at the study of color gradients, we further restrict our spirals to be only face-on galaxies. This restriction is based on two considerations. One is that the internal dust attenuation in the face-on case is minimized. The other is that the *profMean*, which is measured in circular apertures, is more reliable for face-on galaxies. We adopt the criterion $b/a > 0.75$ to make such a face-on selection, where b/a is the axis ratio derived from the exponential profile fitting and given as ab_exp in the SDSS catalog [4] (see EDR paper). We show the histograms of b/a of our sample galaxies in the right panel of

---

[3] In this paper, all the photometric parameters are in the r-band as default unless we specify the other band with a subscript.

[4] Both *fracDeV* and ab_exp are point spread function corrected fitting parameters in the SDSS catalog.

Figure 1. The dotted and solid histograms represent the distributions of galaxies before and after the morphological selection (*fracDeV*< 0.5), respectively. As expected, the b/a shows a flat distribution and parameterizes the inclination of the spiral disk very well (Lambas et al. 1992; Shao et al. 2007). According to the study of Shao et al. (2007), the axis ratio $b/a \sim 0.75$ corresponds to inclination angle $i \sim 41°$ (see fig. 3 of their paper).

Finally, we select a magnitude-limited sample of 25 517 face-on spiral galaxies, whose distributions of *fracDeV* and b/a are shown as shadowed regions in Figure 1.

2.2 Binning and Composing Galaxies

In this section, we describe how to bin sample galaxies and construct *composite* galaxies. To construct a *composite* galaxy, the member galaxies must have similar physical properties. We assume that, if a set of galaxies has similar concentrations (morphological type), physical sizes (angular momentum[5]) and luminosities (stellar mass), their other physical properties are also similar, including the radial color profiles.

We divide the 25 517 sample galaxies into subsamples in small volumes of concentration c, physical half-light radii R_{50} (in units of kpc) and absolute Petrosian magnitudes M. The bin widths of c, R_{50} and M are 0.1, 1.0 kpc and 0.5 mag, respectively. The concentration is defined as $c \equiv R_{90}/R_{50}$, where R_{90} and R_{50} are aperture radii containing 90 and 50 percent of the Petrosian flux (see EDR paper), respectively. The physical size and absolute magnitude are calculated under the cosmology context with $\Omega_0 = 0.3$, $\Omega_\Lambda = 0.7$ and $H_0 = 70 \ \mathrm{km \ s^{-1} \ Mpc^{-1}}$.

After dividing galaxies into subsamples, we measure the dispersion of the colors of all the member galaxies in each subset. This dispersion is very small, with typical value ~ 0.1 mag (comparable to the bin width of the absolute magnitude), which confirms our assumption that all the physical properties of member galaxies are similar when c, R_{50} and M are constrained.

Since the member galaxies of each subset are assumed to have similar color profiles but are located at different redshifts, their color profiles (measured from *profMean* in a series of fixed angular sizes) could be treated as the color measurement of 'one' galaxy at different physical radii. Therefore, the color profile of this *composite* galaxy could be constructed by combining the color profiles of all member galaxies in a subset (e.g., Azzollini et al. 2008; Bakos et al. 2008).

Before we make the composite color profiles, we have made a global K-correction of the color profile of each member galaxy using the routine KCORRECT-V.4.1.4 (Blanton et al. 2003a; Blanton & Roweis 2007). In principle, for each member galaxy, if a color gradient exists, the K-corrections at different radii will be different. This second-order effect has independently been tested by using the *profMean* data of 5 SDSS wavebands to make the K-corrections for each photometric annulus. We found that the difference between the radius dependent K-correction and the global one is less than 0.001 mag.

Figure 2 shows $g - r$ and $r - z$ color profiles of an example *composite* galaxy which comprises 166 member galaxies within the volume of $1.9 < c < 2.0$, $7.0 < R_{50} < 8.0$ kpc and $-21.5 < M < -21.0$ mag. In this figure, each small dot denotes the color in a *profMean* annulus of one member galaxy. These small dots are then divided into 30 bins, with 15 bins inside R_{50} and the others outside. Each inner bin ($R < R_{50}$) contains the same number of data points (average number of all small dots inside R_{50}), as do the outer bins ($R > R_{50}$). We average the colors of small dots in each bin and print them with large circles, with open and filled ones representing the inner and outer ones with R_{50}, respectively. As we can see, by averaging a group of member galaxies, the color profile of the *composite* galaxy tends to be smooth in the sense that the S/N of the color profile has been greatly improved.

To ensure high S/N of the stacked profile, we require the member galaxies in each c-R_{50}-M volume be at least 30. With this constraint, we get 193 *composite* galaxies, containing ~ 80 percent of the initial 25 517 individual galaxies. Those missing galaxies are located in the outskirts of the c-R_{50}-M space with very low number density.

---

[5] At a given magnitude, the galaxies with larger angular momenta (parameterized by larger spin parameter λ) tend to have larger sizes (Mo et al. 1998; Syer et al. 1999).
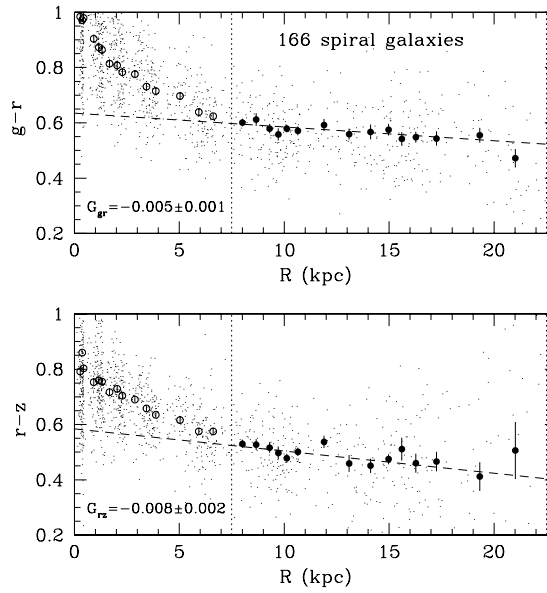
Fig. 2 $g-r$ (*upper panel*) and $r-z$ (*lower panel*) color profiles of an example *composite* galaxy which is composed of 166 member galaxies with $1.9 < c < 2.0$, $7.0 < R_{50} < 8.0$ kpc and $-21.5 < M < -21.0$ mag. Each small dot denotes the color at the radius of the photometric annulus for a member galaxy. The dashed line is the best linear fit of all the small dots between $R_{50} \sim 7.5$ kpc and $3R_{50}$ (denoted by two vertical dotted lines). The large circles show the average color at each of the given radius bins, with open and filled circles separated at R_{50}. The error-bars show the scatters.

2.3 The Color Gradient of the Disk Component

As shown in Figure 2, the color of this *composite* galaxy becomes bluer with increasing radius. The color profile is steeper in the central part and becomes shallower as we move outwards. The outer part of the color profile ($R > R_{50}$) shows a nearly linear shape.

Following the study of Taylor et al. (2005), we separate the color profile of each *composite* galaxy into two parts at R_{50} and consider the region $R > R_{50}$ to be the disk component. We measure the color gradient of the disk component within the region from R_{50} to $3R_{50}$. The outer boundary is based on the considerations that a star formation threshold occurs outside the radius of about 5-times the scale-length R_d ($\sim 3R_{50}$) (van der Kruit & Searle 1981; Pohlen et al. 2000) and large uncertainties in the photometric measurements exist in the very outer regions [6].

Since the color profile of the disk component ($R_{50} \sim 3R_{50}$) can be well parameterized by a straight line, we use the linear least squares fitting to model the gradients of galactic disks. In particular, we make a linear fitting of all the data points in the range $R_{50} \sim 3R_{50}$ and estimate the fitting error with 20 bootstrap samples. The best linear fitting for the example galaxy is shown as the dashed line in Figure 2.

The disk color gradient is then defined as the slope of the fitting line,

$$G_{\rm kpc} = \frac{\Delta \rm CI}{\Delta R(\rm kpc)} \,, \tag{1}$$

where 'CI' is the color index. For our *composite* galaxy, this $G_{\rm kpc}$ can easily be converted to the scaled color gradient, e.g. G_{50} (the color variation per R_{50}), by $G_{50} = G_{\rm kpc} \times R_{50}$, where R_{50} is the average size of member galaxies in each subset.

---

[6] The typical errors of surface brightness at $3R_{50}$ are 0.105 for the g-band, 0.095 for the r-band and 0.273 for the z-band, respectively.

In this paper, we will only present the results of colors $g-r$ and $r-z$. We exclude the colors related to the u band because of its low image sensitivity and high sensitivities to recent star formation and dust attenuation. We do not use the i-band because of the 'Red halo' effect of the Point Spread Function (PSF), which was introduced by Michard (2002) and was first found by Wu et al. (2005) in the SDSS i-band. Except for the i-band, the PSF profiles in the g, r and z bands match each other well (Wu et al. 2005), so the effects of the PSF mismatch on the $g-r$ and $r-z$ color profiles are negligible.

3 RESULTS

3.1 Color Gradient

We measure the color gradients of disks ($R_{50} \sim 3.0R_{50}$) of all 193 *composite* galaxies and show their distributions in Figure 3. Panels (a) and (b) show the histograms of the $g-r$ gradient G_{gr} and the $r-z$ gradient G_{rz}, whereas panels (c) and (d) show the histograms of their errors, respectively.

Consistent with many early studies (e.g., de Jong 1996c; Bell & de Jong 2000; Taylor et al. 2005; Li et al. 2005; Bakos et al. 2008), most of our *composite* galaxies show negative color gradients. We notice that, for the $g-r$ color, about 25 percent have positive gradients. As we will show below, these *composite* galaxies with positive G_{gr} are mainly those with small R_{50} and large uncertainties.

As can be seen in Figure 3, both G_{gr} and G_{rz} show roughly Gaussian distributions with means and scatters $\bar{G}_{gr} = -0.006\,\mathrm{mag\,kpc}^{-1}$, $\bar{G}_{rz} = -0.018\,\mathrm{mag\,kpc}^{-1}$ and $\sigma_{gr} = 0.009$, $\sigma_{rz} = 0.011$. The typical errors of fitted gradients are about 0.003 for G_{gr} and 0.005 for G_{rz}, which are much smaller than the scatters σ_{gr} and σ_{rz}. If we de-convolve these typical errors from the distributions of G_{gr} and G_{rz}, we get intrinsic scatters $\sigma_{gr,i} = 0.008$ and $\sigma_{rz,i} = 0.010$. These non-negligible intrinsic scatters among different *composite* galaxies imply that the color gradient is intrinsically correlated with the physical properties of galaxies. We discuss possible correlations in detail below.
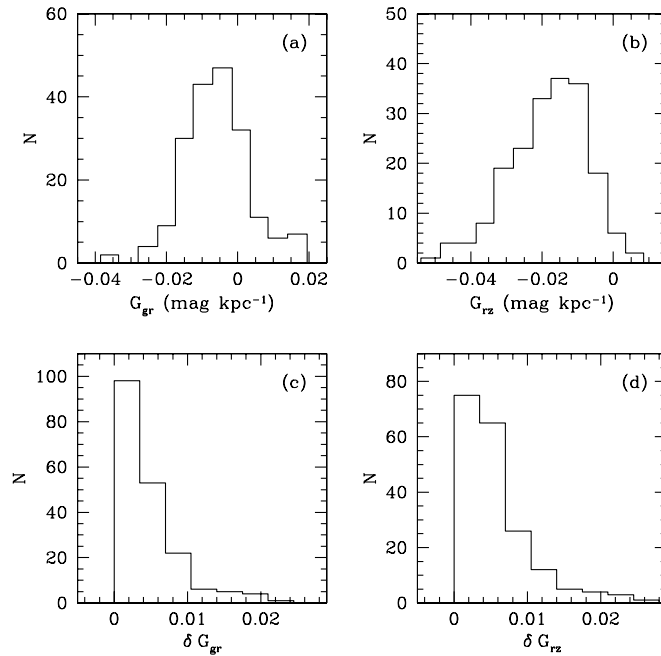
Fig. 3 Distributions of color gradients G_{gr} (a) and G_{rz} (b) of *composite* galaxies. The bottom two panels show the distributions of errors of G_{gr} ($\delta\,G_{gr}$, (c)) and G_{rz} ($\delta\,G_{rz}$, (d)) respectively.
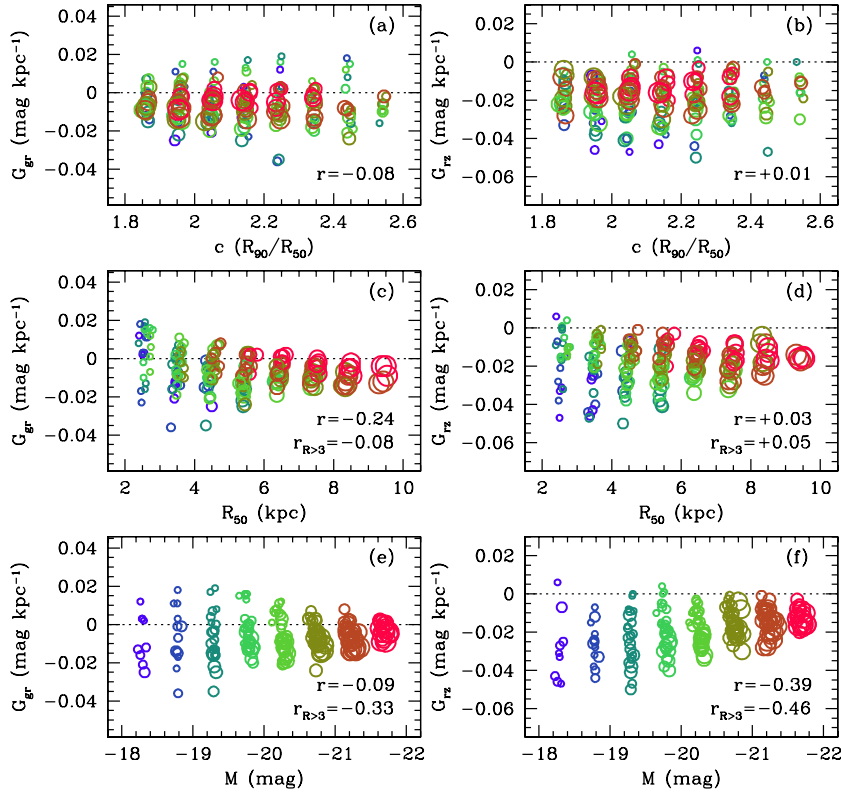
Fig. 4 Color gradients (G_{gr} and G_{rz}) as functions of concentration parameter c, physical half-light radius R_{50} and absolute magnitude M. The correlation coefficients r are labeled in the lower-right corner of each panel. Each point represents the color gradient of one *composite* galaxy. Bigger circles denote galaxies with larger sizes and redder colors represent higher luminosities.

3.2 Correlation with Galaxy Properties

In this section, we study the correlations between the color gradients and structural parameters of galaxies and try to find out which one is the main factor regulating the color gradients. Technically, we use the Pearson's correlation coefficient to quantify each possible correlation[7]. In the case of our sample containing 193 data points, the confidence level of the correlation will be over 99 percent if the absolute value of a correlation coefficient is larger than 0.18.

As described in Section 2.2, our *composite* galaxies are constructed in c-R_{50}-M space, so we first explore the possible correlations between color gradients and these three bin parameters. Figure 4 shows the measured color gradients (G_{gr} and G_{rz}) against the r-band concentration c, physical size R_{50} and absolute magnitude M in the top, middle and bottom panels, respectively. Each circle in the figure represents one *composite* galaxy, with sizes and colors of the circles indicating R_{50} and M of the galaxies. Larger circles represent larger galaxies and redder colors indicate more luminous galaxies. The errors of the color gradients are not shown for clearness (but shown in Fig. 5). The Pearson's correlation coefficients between color gradients and these three parameters (c, R_{50} and M) are labeled in the corner of each panel and listed in Table 1.

---

[7] During the calculation of this coefficient, the error of the color gradient of each *composite* galaxy has been used as a weight.

Table 1 Pearson's correlation coefficients between color gradients (G_{gr} and G_{rz}) and four structural parameters (r-band): concentration parameter c, physical half-light radius R_{50}, absolute magnitude M and disk surface brightness μ_{d}.

	c	R_{50}	M	μ_{d}
G_{gr}	-0.08	$-0.24\ (-0.08^*)$	$-0.09\ (-0.33^*)$	-0.71
G_{rz}	0.01	$0.03\ (0.05^*)$	$-0.39\ (-0.46^*)$	-0.75

Note: * – The correlation coefficients of *composite* galaxies with $R_{50} > 3$ kpc.

3.2.1 With concentration parameter c

As we can see from the top two panels of Figure 4, the color gradients are almost independent of the concentration parameter. The correlation coefficients $r_{G_{\mathrm{gr,\,c}}} = -0.08$ and $r_{G_{\mathrm{rz,\,c}}} = 0.01$ confirm that the color gradients are not correlated with c.

It is well known that the concentration parameter is related to the morphological type, with earlier type galaxies having larger values of c (Shimasaku et al. 2001; Strauss et al. 2002; Nakamura et al. 2003). For spiral galaxies, a larger value of c also indicates an earlier type spiral, i.e. a larger contribution from the bulge component. Therefore, our results imply that the color gradient of the disk component is not related to the bulge. Moreover, this independence of the bulge component also confirms that our separation of the disk component at R_{50} is adequate to avoid the bulge contamination.

3.2.2 With physical size R_{50}

For physical size R_{50}, as can be noticed from the correlation coefficients, the gradient G_{gr} shows a weak correlation ($r_{G_{\mathrm{gr,\,}R_{50}}} = -0.24$), while G_{rz} is independent of R_{50} ($r_{G_{\mathrm{rz,\,}R_{50}}} = 0.03$). If we go to the plot of G_{gr} vs. R_{50} (panel (c) of Fig. 4), we can see that the weak correlation between G_{gr} and R_{50} is mainly caused by the galaxies in the smallest size bin, where more than half of the *composite* galaxies show positive gradients. Actually, if we exclude these galaxies from the correlation analysis, we get a coefficient $r = -0.008$, a similar independent behavior as that of the $r - z$ gradient. Meanwhile, the correlation coefficient $r_{G_{\mathrm{rz,\,}R_{50}}}$ changes from 0.03 to 0.05. We also mention that the measurement of the color gradients of these smallest galaxies is quite uncertain (see the error-bars of these smallest galaxies in Fig. 5) because of the limited number of member galaxies and *profMean* data points. However, the fact that the smallest galaxies show positive G_{gr} but negative G_{rz} may be related to the migrations of star-burst regions in blue compact galaxies (e.g., Schulte-Ladbeck et al. 1999; de Paz & Madore 2005) which is worth studying further.

Another interesting point we can see from the figure is that the dispersion of the color gradients (for both G_{gr} and G_{rz}) tends to be smaller for bigger galaxies. For the biggest galaxy ($R_{50} \sim 9\,\mathrm{kpc}$), the gradients are roughly constants $G_{\mathrm{gr,\,9kpc}} \sim -0.008$ and $G_{\mathrm{rz,\,9kpc}} \sim -0.016$ (where the dispersion is comparable to the measurement error). A similar result has also been found by Muñoz-Mareos et al. (2007), who investigated 161 nearby face-on spiral galaxies and found a smaller $FUV - K$ gradient dispersion for bigger galaxies.

3.2.3 With absolute magnitude M

The correlation coefficients between the color gradients and absolute magnitude are $r_{G_{\mathrm{gr,\,M}}} = -0.09$ and $r_{G_{\mathrm{rz,\,M}}} = -0.39$. Again, when we exclude the *composite* galaxies in the smallest bin size as above, the coefficient $r_{G_{\mathrm{gr,\,M}}}$ increases to -0.33 and $r_{G_{\mathrm{rz,\,M}}}$ becomes -0.46. The weak anti-correlation between the color gradient and absolute magnitude indicates that brighter galaxies have shallower gradients. This result is apparently in conflict with the result of Kim & Ann (1990), where they found more luminous galaxies tend to have steeper color gradients. However, this apparent contradiction is caused by different definitions of the color gradients. Kim & Ann (1990) defined the color gradient as color variation per

scaled radius D_{25}[8], while we adopt the definition of color variation per kpc. As we have mentioned, the color gradient G_{kpc} can be converted to the scaled color gradient by multiplying a factor of physical radius. Since more luminous galaxies have larger sizes (Shen et al. 2003), if we convert G_{kpc} to G_{50}, we also get a positive correlation between G_{50} and absolute magnitude with coefficients 0.17 and 0.18 for the $g - r$ and $r - z$ gradients respectively, i.e. the more luminous galaxies have steeper scaled color gradients.

Until now, we have explored the correlations between the color gradients and three bin parameters separately and found a tendency of lower scatter of color gradients for larger galaxies and a weak correlation between the color gradient and absolute magnitude. If we combine these bin parameters together, we may find more interesting results. In the middle two panels of Figure 4, if we focus on symbol colors, we will find a systematical change that less luminous galaxies (with bluer color symbols) tend to have steeper color gradients in a given radius bin. Similar systematical changes can also be found in the bottom panels of Figure 4, where larger galaxies (with bigger symbol sizes) have steeper color gradients at a given absolute magnitude. These two phenomena indicate a strong correlation between the color gradients and surface brightness. We discuss this correlation in detail below.

3.2.4 With disk surface brightness

In this section, we turn to investigating the correlation between color gradient and disk surface brightness μ_{d}. Here, μ_{d} is defined as the average surface brightness from R_{50} to R_{90} and has been corrected for K-correction and cosmological dimming effect. This definition of the disk surface brightness avoids possible contaminations from the bulge component and is consistent with our measurement of the disk color gradient. We calculate μ_{d} for each member galaxy and then average them to get the disk surface brightness of the *composite* galaxy.
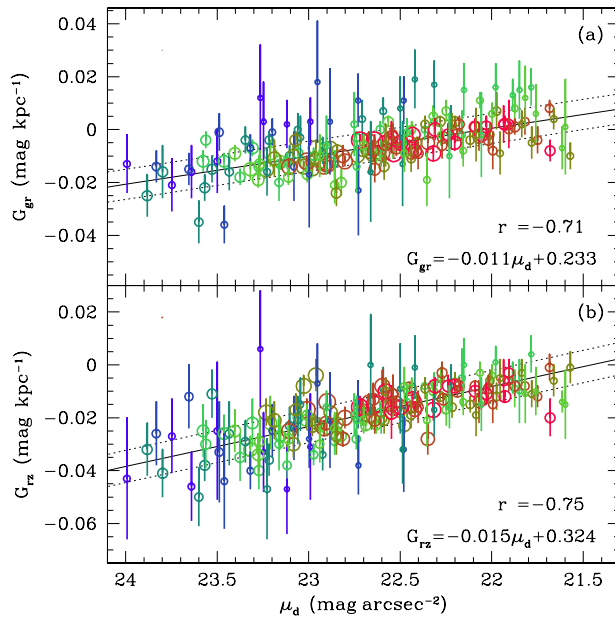
Fig. 5 Relationship between color gradients (G_{gr} and G_{rz}) and disk surface brightness μ_{d}. Each point represents the color gradient of one *composite* galaxy and the error-bar shows the measurement error estimated from bootstrap samples. The solid line in each panel shows the best linear fit of all the data points and the dotted lines represent the region of $\pm 1\sigma$ rms scatter.

---

[8] Kim & Ann (1990) defined the D_{25} as isophotal diameter for $\mu = 25\,\mathrm{mag\,arcsec^{-2}}$ isophote in B-band.

We plot the color gradients against disk surface brightness in Figure 5. Both G_{gr} and G_{rz} show a remarkable anti-correlation with μ_{d}, with correlation coefficients $r_{G_{\mathrm{gr}},\mu_{\mathrm{d}}} = -0.71$ and $r_{G_{\mathrm{rz}},\mu_{\mathrm{d}}} = -0.75$. We use the least squares method to fit linear relations between the color gradients and μ_{d} weighted with the errors of the color gradients. The best fitting results are

$$
\begin{aligned}
G_{\mathrm{gr}} &= -0.011\mu_{\mathrm{d}} + 0.233, \\
G_{\mathrm{rz}} &= -0.015\mu_{\mathrm{d}} + 0.324,
\end{aligned}
\tag{2}
$$

which are shown as the solid lines in Figure 5. The rms (σ) of these fitted relations are 0.005 for G_{gr} and 0.006 for G_{rz}. The range of the $\pm 1\sigma$ region is shown as two dotted lines in each panel. As we can see, most of the galaxies outside the $\pm 1\sigma$ region are small galaxies (small symbol size) with large measurement errors. Moreover, we have tested that the residuals of these best fitting relations are not correlated with either the luminosities or the sizes of galaxies (see the colors and sizes of symbols). That means the weak correlation between the color gradients and absolute magnitude we have found in Section 3.2.3 is actually caused by this $G - \mu_{\mathrm{d}}$ relation and the known $L - \mu_{\mathrm{d}}$ relation (e.g., Shen et al. 2003). This also indicates that the tight correlation between color gradients and disk surface brightness is an intrinsic relation among spiral galaxies, which gives a strong observational constraint on the models of formation and evolution of galactic disks.

4 SUMMARY AND DISCUSSION

In this study, a sample of 25 517 face-on spiral galaxies drawn from SDSS-DR4 is used to investigate the color gradients of galactic disks. We construct *composite* galaxies to improve the S/N of color profiles and measure their color gradients, and then investigate the correlations between the color gradients and structural parameters, including concentration, physical size, luminosity and disk surface brightness. The main results are listed as follows.

1. The color profile of the disk component, from R_{50} to $3R_{50}$, can be well represented by a straight line. Almost all of the *composite* galaxies show negative $r - z$ gradients, while about 75 percent of them show negative $g - r$ gradients. The mean color gradients are $\bar{G}_{\mathrm{gr}} = -0.006\,\mathrm{mag\,kpc}^{-1}$ and $\bar{G}_{\mathrm{rz}} = -0.018\,\mathrm{mag\,kpc}^{-1}$, respectively.
2. The color gradients of galactic disks are independent of morphological type(concentration c).
3. There is also no significant correlation between disk color gradients and the sizes of galaxies (R_{50}), but bigger galaxies tend to have smaller scatters and uncertainties in the color gradients.
4. The color gradients are dependent on the absolute magnitude M, with fainter galactic disks having steeper color gradients. However, this correlation may be caused by the $G - \mu_{\mathrm{d}}$ relation.
5. The most remarkable correlation that we find is between the color gradients and disk surface brightness μ_{d}, which can be fitted by straight lines: $G_{\mathrm{gr}} = -0.011\mu_{\mathrm{d}} + 0.233$ and $G_{\mathrm{rz}} = -0.015\mu_{\mathrm{d}} + 0.324$.

There are two potential causes of color gradients in galactic disks. One is the systematic change of dust attenuation along the disk and the other is the gradient of stellar population.

For dust, a reasonable and simplified assumption is that the dust distribution along the disk is proportional to the stellar mass density profile (e.g., Phillipps & Disney 1988; Regan et al. 2006). Thus, the inner disk contains more dust than the outer region, and naturally generates a negative color gradient (redder as we move inward) as we observed. However, in this scenario, high surface brightness (surface mass density) galaxies have more dust and will generate steeper color gradients than low surface brightness galaxies, which is opposite to our observational results. Therefore, dust attenuation could not be the only cause of the origin of color gradients of galactic disks. Many previous works also have suggested that the dust only plays a minor role in regulating the color gradients of spiral galaxies (e.g., de Jong 1996c; Bell & de Jong 2000; MacArthur et al. 2004; Taylor et al. 2005).

Regarding the stellar population, it is related to the chemical evolution history of the spiral galaxies and has only been studied in detail for local group galaxies (e.g., MW: Chang et al. 1999; Chen et al.

2003; Fu et al. 2009; M31: Yin et al. in preparation; M33: Magrini et al. 2007; Barker & Sarajedini 2008). It is broadly accepted that the star formation rate (SFR) is proportional to the surface mass density (e.g., Bell & de Jong 2000; Kauffmann et al. 2003), and may also be inversely proportional to radius (e.g., Kennicutt 1998; Boissier & Prantzos 1999), which means SFE (star formation efficiency, defined as SFR/Σ_{gas}, where Σ_{gas} is gas surface density) is higher in the inner region than the outer part. Thus, in the inside-out star-forming scenario, the inner regions of galactic disks evolved faster than the outer regions due to higher SFE, leading to older and more metal-rich stellar populations and generating negative color gradients as observed (Prantzos & Boissier 2000, Yin et al. in preparation). Moreover, the Kennicutt star formation law is nonlinearly proportional to the surface brightness as $SFR \propto \mu^{1.4}$ (Kennicutt 1998). So, the higher surface brightness galaxies have higher SFE, i.e. the chemical evolution will be more adequate. Boissier & Prantzos (2000) have modeled the color profiles of galactic disks using a nonlinear star formation law and found that more massive and smaller galaxies (i.e., higher surface density) favor a more rapid early star formation than the lower surface density ones. Their gas fractions are lower and chemical evolutions are more adequate nowadays even in the outer region, which means that the abundance and stellar population vary slowly with radius. Therefore, the color differences between the inner and outer regions of high surface brightness galaxies will be smaller than those of low surface brightness ones. This simple argument concludes a consistent trend with our observational results that the higher surface brightness galaxies have shallower color gradients. However, besides this static chemical evolution, the growth and evolution of galactic disks are related to a lot of complicated processes, e.g. gas cooling, outflow, radial mixing, and minor merging (e.g., Kaiser & Binney 2003; Block et al. 2006). To fully understand and quantify the origin and evolution of color gradients observed in spiral galaxies, more detailed models are required.

References

Abazajian, K., et al. 2004, AJ, 128, 502

Adelman-McCarthy, J. K., et al. 2006, ApJS, 162, 38

Adelman-McCarthy, J. K., et al. 2007, ApJS, 175, 297

Azzollini, R., Trujillo, I., & Beckman, J. E. 2008, ApJ, 679, L69

Bakos, J., Trujillo, I., & Pohlen, M. 2008, ApJ, 683, L103

Barker, M. K., & Sarajedini, A. 2008, MNRAS, 390, 863

Bell, E. F., & de Jong, R. S. 2000, MNRAS, 312, 497

Bernardi, M., Sheth, R. K., Nichol, R.C., Schneider, D. P., & Brinkmann, J. 2005 AJ, 129, 61

Blanton, M. R., et al. 2003a, AJ, 125, 2348

Blanton, M. R., et al. 2003b, ApJ, 594, 186

Blanton, M. R., & Roweis, S. 2007, AJ, 133, 734

Block, D. L., et al. 2006, Nature, 443, 832

Boissier, S., & Prantzos, N. 1999, MNRAS, 307, 857

Boissier, S., & Prantzos, N. 2000, MNRAS, 312, 398

Capaccioli, M., Caon, N., & D'Onofrio, M. 1992, MNRAS, 259, 323

Chang, R. X., Hou, J. L., Shu, C. G., & Fu, C. Q. 1999, A&A, 350, 38

Chang, R. X., Shen, S. Y., Hou, J. L., Shu, C. G., & Shao, Z. Y. 2006, MNRAS, 372, 199

Chen, L., Hou, J. L., & Wang, J. J. 2003, AJ, 125, 1397

Cunow, B. 2004, MNRAS, 353, 477

de Jong, R. S. 1996a, A&AS, 118, 557

de Jong, R. S. 1996b, A&A, 313, 45

de Jong, R. S. 1996c, A&A, 313, 377

de Jong, R. S. 2008, MNRAS, 388, 1521

de Vaucouleurs, G., 1959, Hdb. d. Physik, 53, 311

Desroches, L. B., Quataert, E., Ma, C. P., & West, A. A. 2007, MNRAS, 377, 402

Fu, J., Hou, J. L., Yin, J., & Chang, R. X. 2009, ApJ, 696, 668

Gadotti, D. A., & dos Anjos, S. 2001, AJ, 122, 1298

Gil de Paz, A., & Madore, B. F. 2005, ApJS, 156, 345

Hathi, N. P., Jansen, R. A., Windhorst, R. A., et al. 2008, AJ, 135, 156

Kaiser, C. R., & Biney, J. 2003, MNRAS, 338, 837

Kauffmann, G., et al. 2003, MNRAS, 341, 54

Kennicutt, R. C. Jr. 1998, ApJ, 498, 541

Kim, K. O., & Ann, H. B. 1990, JKAS, 23, 43

Lambas, D. G., Maddox, S. J., & Loveday, J. 1992, MNRAS, 258, 404

Li, H. N., Shao, Z. Y., Xiao, Q. B., & Liu, C. Z. 2005, PABei, 23, 371

Lupton, R., Gunn, J. E., Ivezic, Z., & Knapp, G. R. 2001, ASPC, 238, 269

MacArthur, L. A., Courteau, S., Bell, E., & Holtzman, J. A. 2004, ApJS, 152, 175

Magrini, L., Corbelli, E., & Galli, D. 2007, A&A, 470, 843

Michard, R. 2002, A&A, 384, 763

Mo, H. J., Mao, S., & White, S. D. M. 1998, MNRAS, 295, 319

Moth, P., & Elston, R. J. 2002, AJ, 124, 1886

Muñoz-Mareos, J. C., Gil de Paz, A., Boissier, S., et al. 2007, ApJ, 658, 1006

Nakamura, O., Fukugita, M., Yasud, N., et al. 2003, AJ, 125, 1682

Padilla, N. D., & Strauss, M. A. 2008, MNRAS, 388, 1321

Peletier, R. F., Valentijin, E. A., Moorwood, A. F. M., & Freudling, W. 1994, A&AS, 108, 621

Phillipps, S., & Disney, M. J. 1988, MNRAS, 231, 359

Pohlen, M., Dettmar, R.-J., & Lütticke, R. 2000, A&A, 357, L1

Pohlen, M., & Trujillo, I. 2006, A&A, 454, 759

Prantzos, N., & Boissier, S. 2000, MNRAS, 313, 338

Regan, M. W., et al. 2006, ApJ, 652, 1112

Schulte-Ladbeck, R. E., Hopp, U., Crone, M. M., & Greggio, L. 1999, ApJ, 525, 709

Shao, Z. Y., Xiao, Q. B., Shen, S. Y., Mo, H. J., Xia, X. Y., & Deng, Z. G. 2007, ApJ, 659, 1159

Shen, S. Y., Mo, H. J., White, S. D. M., et al. 2003, MNRAS, 343, 978

Shimasaku, K., et al. 2001, AJ, 122, 1238

Simien, F., & Michard, R. 1990, A&A, 227, 11

Stoughton, C., et al. 2002, AJ, 123, 485(EDR)

Strateva, I., et al. 2001, AJ, 122, 1861

Strauss, M. A., et al. 2002, AJ, 124, 1810

Syer, D., Mao, S., & Mo, H. J. 1999, MNRAS, 305, 357

Tamura, N., & Ohta, K. 2003, AJ, 126, 596

Taylor, V. A., Jansen, R. A., Windhorst, R. A., Rogier, A., Odewahn, S. C., & Hibbard, J. E. 2005, ApJ, 630, 784

van der Kruit, P. C., & Searle, L. 1981, A&A, 95, 105

Wu, H., Shao, Z. Y., Mo, H. J., Xia, X. Y., & Deng, Z. G. 2005, ApJ, 622, 244

York, D., et al. 2000, AJ, 120, 1579

Zhong, G. H., et al. 2008, MNRAS, 391, 986

Zibetti, S., White, S. D. M., & Brinkmann, J. 2004, MNRAS, 347, 556